Nonlinear magnetotransport in dual spin valves

P. Baláž[1] and J. Barnaś[1,2]
[1]*Department of Physics, Adam Mickiewicz University, Umultowska 85, 61-614 Poznań, Poland*
[2]*Institute of Molecular Physics, Polish Academy of Sciences, Smoluchowskiego 17, 60-179 Poznań, Poland*
(Received 26 March 2010; published 28 September 2010)

Recent experiments on magnetoresistance in dual spin valves reveal nonlinear features of electronic transport. We present a phenomenological description of such nonlinear features (current-dependent resistance and giant magnetoresistance) in double spin valves. The model takes into account the dependence of bulk/interface resistance and bulk/interface spin asymmetry parameters for the central magnetic layer on charge current, and consequently on spin accumulation. The model accounts for recent experimental observations.

DOI: 10.1103/PhysRevB.82.104430 PACS number(s): 75.47.De, 72.25.Ba

I. INTRODUCTION

Spin accumulation (spin splitting of the electrochemical potential) is a nonequilibrium phenomenon which is associated with a spatially nonuniform spin asymmetry of two spin channels for electronic transport.[1–3] In the simplest case, it appears at the interface between ferromagnetic and nonmagnetic metals, when current has a nonzero component perpendicular to the interface.[4] Spin accumulation also appears in more complex systems, such as single or double spin valves exhibiting current-perpendicular-to-plane giant magnetoresistance (CPP-GMR) (Refs. 5 and 6) effect, as well as in single or double tunnel junctions. Current-induced spin accumulation is particularly pronounced in spin-polarized transport through nanoparticles[7,8] or quantum dots and molecules.[9]

In the case of spin valves based on layered magnetic structures, spin accumulation and GMR are usually accounted for in terms of the Valet-Fert description,[4,10] in which the spin accumulation is linear in current, while resistance and magnetoresistance are independent of current magnitude and current orientation. The description involves a number of phenomenological parameters which usually are taken from CPP-GMR experimental data. Originally, it was formulated for collinear (parallel and antiparallel) magnetic configurations but later was extended to describe also current-induced spin torque[11] and CPP-GMR for arbitrary noncollinear geometry.[12]

The Valet-Fert description was successfully applied not only to single spin valves, but also to double (dual) spin valves,[13] $F_L/N_L/F_C/N_R/F_R$, where F_C is a magnetically free layer separated from two magnetically fixed outer layers (F_L and F_R) by nonmagnetic spacers (N_L and N_R). An important feature of such structures is an enhanced spin accumulation in the central layer (F_C) for antiparallel magnetizations of the outer magnetic layers (see Fig. 1). Spin accumulation may be then several times larger than in the corresponding single spin valves. Accordingly, such a magnetic configuration of dual spin valves (DSVs) diminishes the critical current needed to switch magnetic moment of the central layer and also enhances the current-induced spin dynamics.[13,14]

Another interesting consequence of the enhanced spin accumulation in the central layer of a dual spin valve is the possibility of nonlinear transport effects. Recent experimental results[15] indicate that the enhanced spin accumulation may cause unusual dependence of magnetoresistance on dc current. It has been shown that when magnetizations of the outer layers are antiparallel, resistance of a DSV for one current orientation is lower when the F_C layer is magnetized along the F_R one and higher when it is aligned along magnetization of the F_L layer while for the opposite current orientation the situation is reversed. Moreover, the difference in resistance of both collinear configurations markedly depends on the applied current. These observations strongly differ from the predictions of the Valet-Fert model,[4] which gives resistance (and magnetoresistance) independent of the current density.

Such a nonlinear behavior may originate from several reasons. The Valet-Fert description is based on the assumption of constant (independent of spin accumulation and current) basic parameters of the model, such as bulk/interface resistance, bulk/interface spin asymmetry, spin-diffusion lengths, etc. This is justified when spin accumulation is small and/or change in the density of states on the energy scale comparable to spin accumulation is negligible in the vicinity of the Fermi level. Density of states can be then considered constant, i.e., independent of energy. Since the density of states determines electron scattering rates, one may safely assume that the transport parameters mentioned above are also constant. However, when the density of states at the Fermi level varies remarkably with energy and spin accumulation is sufficiently large, this assumption may not be valid, and the parameters mentioned above may depend on spin accumulation.[15] This, in turn, may lead to nonlinear effects, such as the experimental ones described above.[15]

The spin accumulation, however, is rather small—on the order of 0.1 meV for current density of 10^8 A/cm^2. Thus, to account for the experimental observations one would need

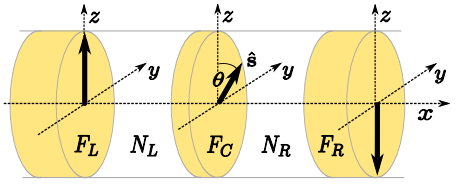

FIG. 1. (Color online) Scheme of a dual spin valve with antiparallel configuration of outer magnetic layers, F_L and F_R. F_C is the central magnetic layer.

rather large gradient of the density of states with respect to energy at the Fermi level. More specifically, to account the experimental observations, the change in density of states should be on the order of 10% on the energy scale of 1 meV. Although this is physically possible, one cannot exclude other contributions to the effect. Spin accumulation can directly change effective scattering potential for electrons at the Fermi level. Moreover, spin accumulation can also indirectly influence transport parameters, for instance, via current-induced shift of the energy bands due to charging of the layers or due to electron correlations, which are neglected in the description of the spin accumulation. Since the experimental results show that the nonlinear effects appear only in the antiparallel configuration, where spin accumulation in the central layer is large, we assume that the indirect contributions are proportional to spin accumulation (at least in the first order). Since, it is not clear which contribution is dominant, we present a phenomenological approach, which effectively includes all contributions to the observed nonlinear transport. We assume that bulk and interfacial resistances as well as spin asymmetries vary with spin accumulation and show that such variation leads to effects comparable to experimental observations.[15]

Structure of this paper is as follows. In Sec. II we describe the model. Numerical results are presented in Sec. III for bulk and interfacial contributions. Section IV deals shortly with magnetization dynamics in DSV. Finally, we conclude in Sec. V.

II. MODEL

Electron-scattering rate and its spin asymmetry become modified when the spin-dependent Fermi levels are shifted (e.g., due to spin accumulation). All the effects leading to this modification can be included in the description of charge and spin transport presented in Refs. 11 and 12, which generalize the Valet-Fert model to noncollinear magnetic configurations. We analyze the situation when the effect originates from the bulk resistivity and bulk spin asymmetry factor β of the F_C layer, which are assumed to depend on spin accumulation, as well as from similar dependence of the corresponding interface parameters. Let us begin with the bulk parameters.

The spin-dependent bulk resistivity of a magnetic layer is conveniently written in the form[4]

$$\rho_{\uparrow(\downarrow)} = 2\rho^*(1 \mp \beta), \tag{1}$$

where ρ^* is determined by the overall bulk resistivity ρ_F as $\rho^* = \rho_F/(1-\beta^2)$. When the spin accumulation is sufficiently large, one should take into account the corresponding variation in ρ^*. In the lowest approximation (linear in the spin accumulation) one can write

$$\rho^* = \rho_0^* + q\langle g\rangle, \tag{2}$$

where ρ_0^* is the corresponding *equilibrium* (zero-current limit) value, and $g(x)$ is spin accumulation in the central layer, which varies with the distance from layer's interfaces. To disregard this dependence, we average the spin accumulation over the layer thickness $\langle g\rangle = (1/d)\int_{F_C} g(x)dx$. In Eq. (2) q is a phenomenological parameter, which depends on the relevant band structure. This parameter effectively includes all effects leading to the modification of transport parameters.

This equation can be rewritten as

$$\rho^* = \rho_0^*(1 + \tilde{q} i\langle\tilde{g}\rangle), \tag{3}$$

where $\tilde{g}$ is a dimensionless variable related to spin accumulation, $\tilde{g} = (e^2 j_0 \rho_0^* l_{sf})^{-1} g$, with j_0 denoting the particle current density and l_{sf} being the spin-flip length. We also introduced the dimensionless current density $i = I/I_0$ with $I = ej_0$ denoting the charge current density and I_0 being a current density scale typical for metallic spin valves ($I_0 = 10^8$ A/cm^2). The parameter $\tilde{q}$ in Eq. (3), $\tilde{q} = (eI_0 l_{sf})q$, is a dimensionless phenomenological parameter which is independent of current.

The bulk spin-asymmetry parameter β becomes modified by spin accumulation as well and this modification can be written in a form similar to that in the case of ρ^*, i.e.,

$$\beta = \beta_0 + \xi\langle g\rangle, \tag{4}$$

where β_0 is the corresponding equilibrium value and ξ effectively includes all the contributions. When introducing the dimensionless spin accumulation defined above, one can rewrite Eq. (4) as

$$\beta = \beta_0 + \tilde{\xi} i\langle\tilde{g}\rangle, \tag{5}$$

where $\tilde{\xi} = (eI_0\rho_0^* l_{sf})\xi$.

Similar equations can be written for the interfacial resistance R^* and interfacial asymmetry parameter γ, which define spin-dependent interface resistance as

$$R_{\uparrow(\downarrow)} = 2R^*(1 \mp \gamma). \tag{6}$$

Analogously, we can write the dependence of R^* and γ on spin accumulation in the form

$$R^* = R_0^* + q' g(x_i), \tag{7a}$$

$$\gamma = \gamma_0 + \xi' g(x_i), \tag{7b}$$

where $g(x_i)$ is spin accumulation at a given interface. The constants R_0^* and γ_0 are equilibrium interfacial resistance and asymmetry parameter, respectively. Relations in Eq. (7) lead to the following dependence of the interfacial parameters on the current density:

$$R^* = R_0^*[1 + \tilde{q}' i\tilde{g}(x_i)], \tag{8a}$$

$$\gamma = \gamma_0 + \xi' i\tilde{g}(x_i), \tag{8b}$$

where $\tilde{q}' = (eI_0\rho_0^* l_{sf})q'$ and $\tilde{\xi}' = (eI_0\rho_0^* l_{sf})\xi'$.

The parameters q, ξ, q', and ξ' introduced above describe deviation from usual behavior of the resistance (magnetoresistance) described by the Valet-Fert model. These parameters will be considered as independent phenomenological ones.

TABLE I. Bulk parameters used in calculations.

Material	ρ^* ($\mu\Omega$ cm)	β	l_{sf} (nm)
Co	5.1	0.51	60
Py	16	0.77	5.5
Cu	0.5	0	350
IrMn	150	0	1

III. NUMERICAL RESULTS

To calculate resistance and spin accumulation for arbitrary noncollinear magnetic configuration, we apply the formalism described in Refs. 11 and 12. This formalism, however, is modified by assuming ρ^*, β, R^*, and γ to depend on current density (spin accumulation). Therefore, for a particular magnetic configuration and for certain values of i, $\tilde{q}$, $\tilde{\xi}$, $\tilde{q}'$, and $\tilde{\xi}'$, the spin accumulation has to be calculated together with ρ^*, R^*, β, and γ in a self-consistent way. In the first step, we assume equilibrium values; $\rho^*=\rho_0^*$ and $\beta=\beta_0$ ($R^*=R_0^*$ and $\gamma=\gamma_0$), and calculate the corresponding spin accumulation $g_0(x)$ in the central magnetic layer. Then, we calculate the zero approximation of the out-of-equilibrium parameters according to Eqs. (3), (5), and (8). With these new values for ρ^* and β (R^* and γ) we calculate the out-of-equilibrium spin accumulation in the central layer and *new* out-of-equilibrium values of ρ^* and β (R^* and γ). The iteration process is continued until a stable point is reached. Finally, for the obtained values of ρ^*, β, R^*, γ, and spin accumulation, we calculate the resistance R of the DSV at a given magnetic configuration (see Ref. 12).

In all our calculations, magnetizations of the outermost layers are assumed to be fixed and antiparallel (like in experiment in Ref. 15). Current is defined as positive for electrons flowing from F_R toward F_L. The equilibrium parameters have been taken from the relevant literature[16] (Tables I and II).

In this section we apply the above described model to two examples of DSV structures. The first one is a symmetric DSV with $F_L=F_R=$Co(20 nm), $F_C=$Py(8 nm), and with the magnetic layers separated by 10-nm-thick Cu spacers. The second considered structure is an asymmetric exchange-biased DSV similar to that used in experiment,[15] namely, Cu-Co(6)/Cu(4)/Py(2)/Cu(2)/Co(6)/IrMn(10)-Cu, where the numbers in brackets correspond to layer thicknesses in nanometers.

TABLE II. Interfacial parameters used in calculations; R^* is given in fΩ m^2, and mixing conductance, $G_{\uparrow\downarrow}$, in (fΩ m^2)$^{-1}$. Only parameters needed in calculations are given.

Interface	R^*	γ	Re$\{G_{\uparrow\downarrow}\}$	Im$\{G_{\uparrow\downarrow}\}$
Co/Cu	0.5	0.77	0.542	0.016
Py/Cu	0.5	0.70	0.390	0.012
Co/IrMn	0.5	0.10		
IrMn/Cu	0.5	0.70		

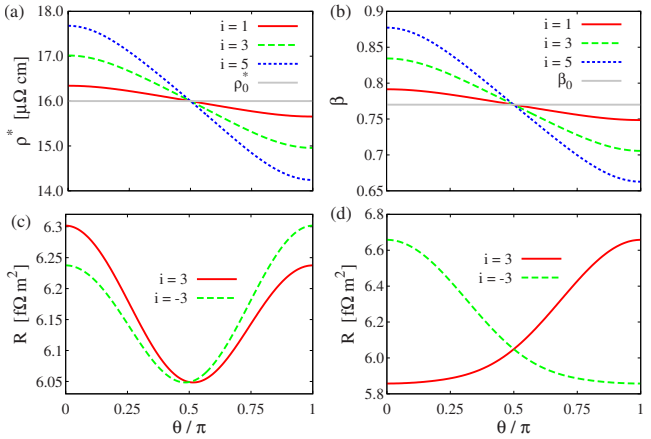

FIG. 2. (Color online) Symmetric dual spin valve Cu-Co(20)/Cu(10)/Py(8)/Cu(10)/Co(20)-Cu: (a) angular dependence of ρ^* for $\tilde{q}=0.1$ and $\tilde{\xi}=0$; (b) angular dependence of β for $\tilde{\xi}=0.1$ and $\tilde{q}=0$; (c) angular dependence of the resistance (per unit square) for $\tilde{q}=0.1$ and $\tilde{\xi}=0$; and (d) angular dependence of the resistance for $\tilde{\xi}=0.1$ and $\tilde{q}=0$. The relative current density i as indicated.

A. Bulk effects

In this section we consider pure bulk effects assuming $\tilde{q}'=0$ and $\tilde{\xi}'=0$. We start from a symmetric DSV and the corresponding numerical results are shown in Fig. 2. First, we analyze the case with $\tilde{q}=0.1$ and $\tilde{\xi}=0$. Figure 2(a) shows how ρ^* varies when magnetization of the central layer is rotated in the layer plane. This rotation is described by the angle θ between magnetizations of the F_L and F_C layers. The higher the current density, the more pronounced is the deviation of ρ^* from its equilibrium value ρ_0^*. The current-induced change in ρ_0^* reaches maxima when magnetic moment of the central layer is collinear with those of the outer layers. These maxima are different for the two opposite orientations of the magnetic moment of F_C layer, as the corresponding spin accumulations are different. For $\theta=\pi/2$, however, one finds $\rho^*=\rho_0^*$. This is because spin accumulation vanishes then due to opposite contributions of both interfaces (for symmetric DSVs). Variation of ρ^* in Fig. 2(a) is shown only for positive current, $i>0$. When current is negative, the change in ρ^* due to spin accumulation changes sign (not shown), as also can be concluded from Fig. 2(c).

The current-induced angular dependence of ρ^* makes the resistance of the DSV dependent on the current density. As shown in Fig. 2(c), the angular dependence of the resistance becomes asymmetric, i.e., its magnitudes in the opposite collinear states ($\theta=0$ and π) are different. Such an asymmetric angular dependence qualitatively differs from that obtained from the Valet-Fert description, where the resistance is symmetric. When magnetization of the central layer switches (e.g., due to an applied magnetic field) from one collinear state to the opposite one, one finds a drop (positive or negative) in the resistance, defined as $\Delta R=R(\theta=\pi)-R(\theta=0)$. Moreover, when the current direction is reversed, the corresponding drop in resistance also changes sign, as shown in Fig. 2(c).

Let us consider now the situation where β changes with the spin accumulation (current), while ρ^* is constant, $\tilde{\xi}=0.1$

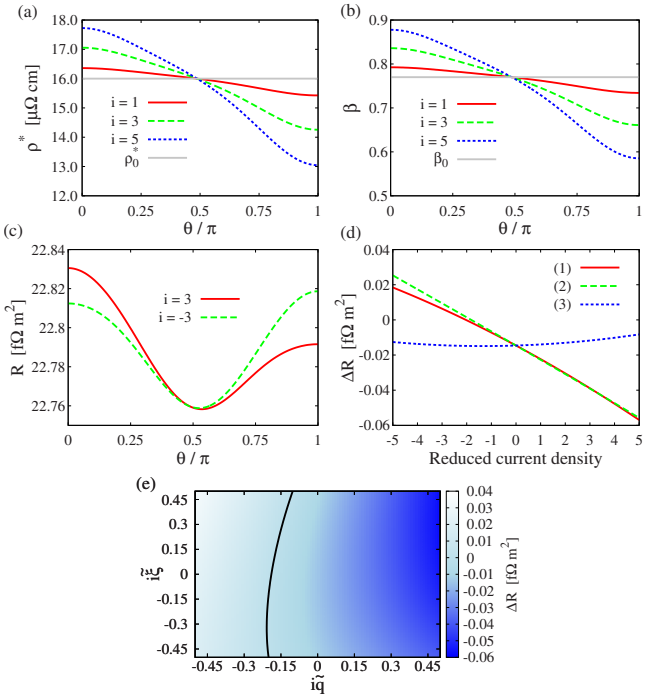

FIG. 3. (Color online) Asymmetric exchange-biased dual spin valve Cu-Co(6)/Cu(4)/Py(2)/Cu(2)/Co(6)/IrMn(10)-Cu: angular dependence of ρ^* (a) and β (b) for $\tilde{q}=0.1$ and $\tilde{\xi}=0.1$, and the angular dependence of the corresponding resistance (c); (d) dependence of the drops in resistance (per unit square) as a function of the reduced current density i for $\tilde{q}=0.1$, $\tilde{\xi}=0.1$ [line (1)], $\tilde{q}=0.1$, $\tilde{\xi}=10^{-3}$ [line (2)], and $\tilde{q}=10^{-3}$, $\tilde{\xi}=0.1$ [line (3)]; and (e) drop in the resistance as a function of $i\tilde{q}$ and $i\tilde{\xi}$ (with reduced current density i); the line covers the points where $\Delta R=0$.

and $\tilde{q}=0$. General behavior of β and of the corresponding resistance with the angle θ is similar to that discussed above [see Figs. 2(b) and 2(d)], although the sign of the resistance drop for the current of a given orientation is now opposite to that obtained in the case discussed above, compare Figs. 2(c) and 2(d). Generally, the sign of the drop in resistance may be controlled by the parameters $\tilde{\xi}$ and $\tilde{q}$.

In real structures, however, both parameters, $\tilde{\xi}$ and $\tilde{q}$, may be different from zero, and the observed behavior results from interplay of the bulk and interface effects discussed above. To show this, we consider now an asymmetric exchange-biased DSV structure, Cu-Co(6)/Cu(4)/Py(2)/Cu(2)/Co(6)/IrMn(10)-Cu, similar to that studied experimentally.

Figures 3(a) and 3(b) show the current-induced angular dependence of ρ^* and β for $\tilde{q}=\tilde{\xi}=0.1$. In comparison to the symmetric DSV structure, the difference in the deviations of both parameters from their equilibrium values for $\theta=\pi$ and $\theta=0$ is now much more pronounced. As before, the nonequilibrium values of the parameters cross the corresponding equilibrium ones for nearly perpendicular configuration, $\theta \approx \pi/2$. The resistance shown in Fig. 3(c) reveals well-defined drop between both collinear configurations, and the drop changes sign when the current is reversed. However, the resistance drops are now different in their absolute magnitude due to the asymmetry of DSV.

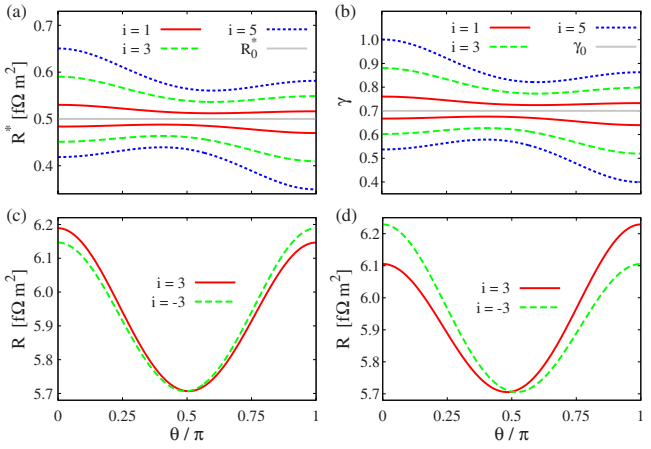

FIG. 4. (Color online) Symmetric dual spin valve Cu-Co(20)/Cu(10)/Py(8)/Cu(10)/Co(20)-Cu: (a) angular dependence of R^* on the left (curves below R_0^*) and right (curves above R_0^*) interfaces of the central layer for $\tilde{q}'=0.1$ and $\tilde{\xi}'=0$; (b) angular dependence of γ on the left (curves below γ_0) and right (curves above γ_0) interfaces of the central layer for $\tilde{\xi}'=0.1$ and $\tilde{q}'=0$; (c) angular dependence of the resistance (per unit square) for $\tilde{q}'=0.1$ and $\tilde{\xi}'=0$; and (d) angular dependence of the resistance (per unit square) for $\tilde{\xi}'=0.1$ and $\tilde{q}'=0$.

Figure 3(d) shows the resistance drops as a function of the current density for three different sets of parameters. For the parameters used in Figs. 3(a)–3(c), i.e., for $\tilde{q}=\tilde{\xi}=0.1$ [line (1)], the absolute value of the drop increases rather linearly with increasing magnitude of current, although the growth of ΔR is faster for positive than for negative current. In the second case, $\tilde{q}=0.1$ and $\tilde{\xi}=10^{-3}$ [line (2)], the dependence remains nearly the same, with only a small deviation from the first case. Finally, we reduced the parameter $\tilde{q}$, $\tilde{q}=10^{-3}$, while $\tilde{\xi}=0.1$ [line (3)]. Now, the dependence strongly differs from the first two cases. ΔR only slightly varies with current and remains rather small. Such a behavior results from interplay of the bulk and interface contributions. This interplay is presented also in Fig. 3(e), where the resistance drop is shown as a function of $i\tilde{q}$ and $i\tilde{\xi}$. Additionally, the latter figure shows that for any value of $\tilde{q}$ there is a certain value of $\tilde{\xi}$ for which $\Delta R=0$ (presented by the line).

B. Interfacial effects

Now we consider the nonlinear effects due to current-dependent interfacial parameters, as given by Eqs. (8). For both symmetric and asymmetric spin valves we assume that the parameters $\tilde{q}'$ and $\tilde{\xi}'$ are equal for both interfaces of the central layer. Consider first a symmetric DSV. The corresponding results are summarized in Fig. 4. Variation in R^*, when the central magnetization rotates in the layer plane, is shown in Fig. 4(a) for $\tilde{q}'=0.1$ and $\tilde{\xi}'=0$. The curves below the equilibrium value R_0^* correspond to R^* on the left interface while these above R_0^* describe R^* on the right interface. When the central magnetization is close to the collinear orientation $(\theta=0,\pi)$, R^* on the left and right interfaces are

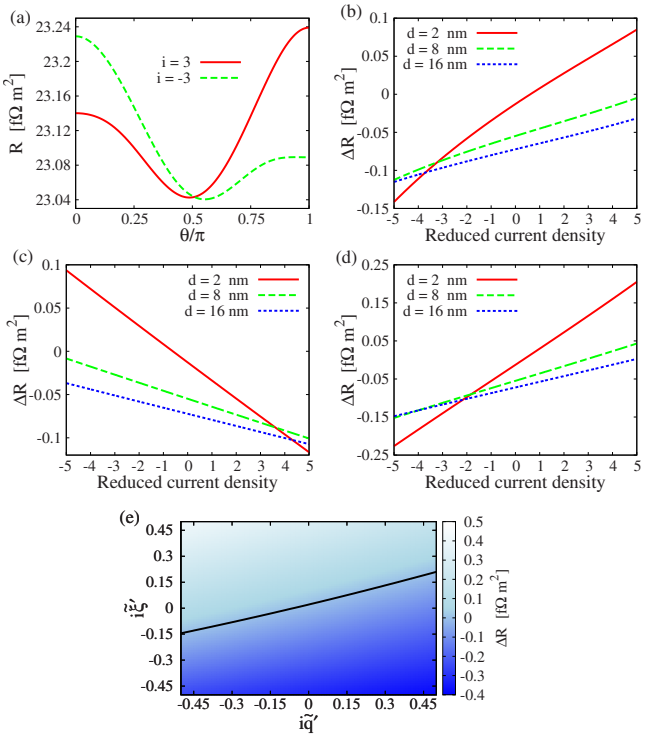

FIG. 5. (Color online) Asymmetric exchange-biased dual spin valve Cu-Co(6)/Cu(4)/Py(d)/Cu(2)/Co(6)/IrMn(10)-Cu: (a) angular dependence of resistance (per unit square) calculated for central layer thickness $d=2$ nm, $\tilde{q}'=0.1$, and $\tilde{\xi}'=0.1$; (b) dependence of the resistance drop (per unit square) on the reduced current density i for $\tilde{q}'=0.1$, $\tilde{\xi}'=0.1$, and for different values of d; (c) resistance drop as a function of the reduced current density i for $\tilde{q}'=0.1$, $\tilde{\xi}'=10^{-3}$, and indicated values of d; (d) resistance drop vs current density i for $\tilde{\xi}'=0.1$, $\tilde{q}'=10^{-3}$, and for indicated values of d; and (e) resistance drop as a function of $i\tilde{q}'$ and $i\tilde{\xi}'$, calculated for $d=2$. The line in (e) covers the points where $\Delta R=0$.

significantly different, and this difference becomes partly reduced when θ tends to $\theta=\pi/2$ (for the systems considered). Generally, the higher current density, the more pronounced is the shift of R^* on both interfaces from their equilibrium values. The corresponding angular dependence of the DSV resistance is shown in Fig. 4(c) for the current densities $I/I_0=\pm 3$. This angular dependence results in small resistance drops of opposite signs for opposite currents. As shall be shown below, the small value of ΔR is due to a relatively large thickness of the central layer. Similar conclusions can also be drown in the case when $\tilde{q}'=0$ and only γ depends on spin accumulation, as shown in Figs. 4(b) and 4(d).

For the asymmetric exchange-biased DSVs, we assume that both R^* and γ depend on spin accumulation. As shown in Fig. 5(a) for $\tilde{q}'=\tilde{\xi}'=0.1$, there is a relatively large drop in resistance for the assumed parameters. This resistance drop ΔR increases rather linearly with the current density, as shown in Fig. 5(b). A small deviation from the linear behavior can be observed only for larger values of negative current. Calculations for different thicknesses of the central layer, $d=2$, 8, and 16 nm, show that the slope of the curves representing the resistance drop as a function of the current density decreases as the thickness increases, see Fig. 5(b). In other words, the dependence of resistance on current becomes less pronounced when the central layer is thicker. We note, that such behavior was not observed in the case of the bulk contribution. This feature arises because for thicker magnetic layers the bulk resistivity dominates the pillar resistance and suppresses the current-induced effects due to interfaces. Additionally, the slope of the curves presenting the resistance drop as a function of current density depends on the parameters $\tilde{q}'$ and $\tilde{\xi}'$, and can change sign for appropriate values of these parameters. This is shown in Figs. 5(c) and 5(d), where one of the parameters, either $\tilde{\xi}'$ (c) or $\tilde{q}'$ (d) has been reduced to 10^{-3}. Since $\tilde{q}'$ and $\tilde{\xi}'$ are of the same sign, their effects are opposite and the corresponding contributions may partly compensate each other. This is also shown in Fig. 5(e), where the resistance drop ΔR is shown as a function of $i\tilde{q}'$ and $i\tilde{\xi}'$. From this figure also follows that total compensation of the contributions to the resistance drop occurs for the points corresponding to the line in Fig. 5(e).

IV. MAGNETIZATION DYNAMICS

In the analysis presented above magnetization of the central layer was in the layer plane. However, when the magnetization switches between the two collinear orientations (due to applied magnetic field), it precesses and comes into out-of-plane orientations as well. Such a precessional motion modifies spin accumulation and also DSV's resistance. In this section we describe variation of the resistance, when magnetization of the central layer is switched by an external magnetic field back and forth. To do this we make use of the single-domain approximation. We also assume that the magnetic field is applied along the easy axis of the central layer, similarly as in experiment (see Fig. 1).

Time evolution of the spin moment of central layer is described by the Landau-Lifshitz-Gilbert equation

$$\frac{d\hat{\boldsymbol{s}}}{dt} = -|\gamma_g|\mu_0\hat{\boldsymbol{s}} \times \boldsymbol{H}_{\text{eff}} + \alpha\hat{\boldsymbol{s}} \times \frac{d\hat{\boldsymbol{s}}}{dt}. \tag{9}$$

Here $\hat{\boldsymbol{s}}$ is a unit vector along the spin moment of the central layer, γ_g is gyromagnetic ratio, μ_0 vacuum permeability, α is a dimensionless damping parameter, and $\boldsymbol{H}_{\text{eff}}$ stands for effective magnetic field,

$$\boldsymbol{H}_{\text{eff}} = -H_{\text{ext}}\hat{\boldsymbol{e}}_z - H_{\text{ani}}(\hat{\boldsymbol{s}}\cdot\hat{\boldsymbol{e}}_z)\hat{\boldsymbol{e}}_z + \boldsymbol{H}_{\text{dem}} + \boldsymbol{H}_{\text{th}}, \tag{10}$$

which includes external magnetic field (H_{ext}) applied along $\hat{\boldsymbol{e}}_z$ axis (see Fig. 1), anisotropy field (H_{ani}), and demagnetization field ($\boldsymbol{H}_{\text{dem}}$) calculated for a layer of thickness $d=2$ nm and elliptical shape with the major and minor axes 130 nm and 60 nm, respectively. $\boldsymbol{H}_{\text{th}}$ is a stochastic Gaussian field with dispersion $D=(\alpha k_B T)/(\gamma_g \mu_0^2 M_s V)$, which describes thermal fluctuations at temperature T, where k_B is the Boltzmann constant, and V is volume of the central magnetic layer. Magnetic moments of the outer layers are assumed to be fixed due to much larger coercive fields of these layers. Moreover, the torque due to spin transfer has not been included.

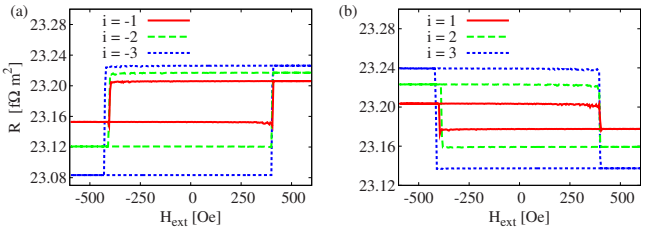

FIG. 6. (Color online) Asymmetric exchange-biased dual spin valve Cu-Co(6)/Cu(4)/Py(2)/Cu(2)/Co(6)/IrMn(10)-Cu: Minor hysteresis loops of resistance in external magnetic field calculated for $\tilde{q}'=0.1$, $\tilde{\xi}'=0.1$, and for different current densities i. Only interface contribution is considered here.

Figure 6 shows quasistatic minor hysteresis loops of the resistance in external magnetic field, calculated for asymmetric exchange-biased DSV at $T=70$ K. These figures are in agreement with the results obtained in the preceding section and also in good agreement with experimental observations.[15] They also show that the drop in resistance changes sign when the direction of current is reversed. Moreover, one can observe small salient points in the hysteresis loops, which appear during the reversal process—especially at low current densities. These points indicate on the minima in resistance at noncollinear configurations and have been observed experimentally as well.

The minor hysteresis loops appear also in the case when the nonlinear effect is due to bulk parameters (not shown). Some differences however appear, for instance, in their dependence on the layer thickness. This suggests that the experimentally observed effects are more likely due to interface contribution, which is quite reasonable as the spin accumulation is maximal just at the interfaces.

V. CONCLUSIONS AND DISCUSSION

In summary, we have extended the description of spin accumulation and magnetotransport in order to account for nonlinear magnetotransport in metallic spin valves. We assumed the dependence of bulk resistivities, interface resistances, and bulk/interface asymmetry parameters on spin accumulation in the central layer. The assumed phenomenological parameters effectively include different contributions leading to modification of the spin-dependent density of states at the Fermi levels. The obtained numerical results reflect the trends observed experimentally. More specifically, the dependence on spin accumulation of any of the considered parameters leads to an asymmetric modification of spin-valve resistance in comparison to its equilibrium (zero-current) value. This modification results in a drop in resistance when the magnetic moment of the central layer switches between two collinear configurations. Moreover, this drop depends on the current density, as has been also shown in experiment.[15] Within our phenomenological description we can reproduce mainly linear dependence of the current-induced resistance drops with a small deviation from the linearity for higher current densities. However, the description fails to account strongly nonlinear variation in ΔR, which was observed in some DSV structures at high current densities.[15] To account for this behavior one should take into account higher order terms in the expansion of the relevant parameters. Additionally, when only interfacial contribution is taken into account, the dependence of ΔR on current becomes less pronounced with increasing thickness of the central layer. Such a behavior has been observed experimentally,[15] too, which indicates that the interface contribution to the nonlinear effects is more important than the bulk one.

The resistance drop measured experimentally at the current density of $I=10^7$ A cm^{-2} is about 0.04 fΩ m^2. To reach effects of similar magnitude within the interfacial model, as shown in Fig. 5, one needs $\tilde{\xi}'\sim 1$, i.e., $\xi \simeq 1.13$ (meV)$^{-1}$ (when assuming the effect is due to variation of interfacial asymmetry parameter only). If direct contribution from spin accumulation would dominate, then the corresponding change in the density of states would be of the order of 10% on the energy scale of 1 meV. This slope may be much smaller in the presence of other contributions.

ACKNOWLEDGMENTS

The work has been supported by the EU through the Marie Curie Training Network SPINSWITCH (Grant No. MRTN-CT-2006-035327). Authors thank Martin Gmitra for helpful discussions.

[1] P. C. van Son, H. van Kempen, and P. Wyder, Phys. Rev. Lett. **58**, 2271 (1987).
[2] M. Johnson and R. H. Silsbee, Phys. Rev. B **37**, 5326 (1988).
[3] A. Barthélémy *et al.*, J. Magn. Magn. Mater. **242-245**, 68 (2002).
[4] T. Valet and A. Fert, Phys. Rev. B **48**, 7099 (1993).
[5] J. Bass and W. P. Pratt, J. Magn. Magn. Mater. **200**, 274 (1999).
[6] J. A. Katine, F. J. Albert, R. A. Buhrman, E. B. Myers, and D. C. Ralph, Phys. Rev. Lett. **84**, 3149 (2000).
[7] J. Barnaś and A. Fert, Phys. Rev. Lett. **80**, 1058 (1998).
[8] A. Brataas, Y. V. Nazarov, J. Inoue, and G. E. W. Bauer, Phys. Rev. B **59**, 93 (1999).
[9] W. Rudziński and J. Barnaś, Phys. Rev. B **64**, 085318 (2001).
[10] V. S. Rychkov, S. Borlenghi, H. Jaffres, A. Fert, and X. Waintal, Phys. Rev. Lett. **103**, 066602 (2009).
[11] J. Barnaś, A. Fert, M. Gmitra, I. Weymann, and V. K. Dugaev, Phys. Rev. B **72**, 024426 (2005).
[12] M. Gmitra and J. Barnaś, Phys. Rev. B **79**, 012403 (2009).
[13] L. Berger, J. Appl. Phys. **93**, 7693 (2003).
[14] P. Baláž, M. Gmitra, and J. Barnaś, Phys. Rev. B **80**, 174404 (2009).
[15] A. Aziz, O. P. Wessely, M. Ali, D. M. Edwards, C. H. Marrows, B. J. Hickey, and M. G. Blamire, Phys. Rev. Lett. **103**, 237203 (2009).
[16] M. Gmitra and J. Barnaś, in *Toward Functional Nanomaterials*, edited by Z. Wang (Springer, New York, 2009), pp. 285–322.